ORBITAL MANEUVERS OF A LUNAR ARTIFICIAL SATELLITE, UNDER THE ACTION OF GRAVITATIONAL AND NON-GRAVITATIONAL PERTURBATION FORCES

Liana Dias Gonçalves[(1)], **Evandro Marconi Rocco**[(2)], **and Rodolpho Vilhena de Moraes**[(3)]
[(1)(2)] National Institute for Space Research (INPE), Av. dos Astronautas, 1758, São José dos Campos, Brazil, lianadgon@gmail.com, evandro.rocco@inpe.br
[(3)]Universidade Federal de São Paulo, São José dos Campos, Brasil, rodolpho.vilhena@gmail.com

Abstract: *The objective of this study is to analyze the orbital maneuvers of an artificial satellite around the Moon surface subject to perturbative forces of gravitational and not gravitational origin, such as lunar gravitational potential, gravitational attraction of the Earth and the Sun, lunar albedo and solar radiation pressure. Optimal maneuvers were obtained from the Lambert's problem solution (Two Point Boundary Value Problem) in order that is minimized the fuel consumption. Then a selected maneuver was simulated assuming a more realistic model of the propulsion system. For both cases is analyzed the actions of thrusters, fuel consumption and deviations in the orbital elements that characterize the lunar orbit of artificial satellite. The deviation is obtained by a comparison between the actual state and the reference state of the vehicle at each step of the simulation. The actual state is calculated every step of the simulation and the reference state is determined considering the desired final orbital elements for the trajectory.*

Keywords: *Astrodynamics, Orbital Maneuvers, Continuous Thrust, Perturbations.*

1. Introduction

An artificial satellite orbiting the lunar surface is subject to disturbances that can cause changes in their orbital motion. These disturbances can be of gravitational origin, as the lunar gravitational potential and the gravitational attraction of other bodies, like the Earth and the Sun; or non-gravitational origin, like lunar albedo and solar radiation pressure.
All perturbations are studied, modeled and implemented in a simulator called Spacecraft Trajectory Simulator - STRS, which allows controlling the trajectory so that deviations and errors in the state variables are minimized.
This work is divided into three stages: the first makes an analysis of the mentioned perturbations, aiming to study the magnitude of such forces and their ability to disturb the satellite and vary the orbital elements. In the second step, a calculation of an orbital maneuver is done by connecting the satellite from an initial position to the final desired position using the two point boundary value problem. Finally, we propose an innovative approach that uses an automatic control system that connects an initial orbit to a final orbit using continuous propulsion and trajectory control in closed loop.
The orbital motion can be determined by solving Kepler's equation at each step defined as an input parameter in the simulator (STRS). The lunar gravitational potential can be expressed by the expansion of normalized spherical harmonic coefficients, as a function of gravitational

constant, of lunar equatorial radius, of distance from the satellite to the Moon, of the latitude and longitude and of the normalized Legendre associated polynomials.
The dynamics of the movement of a n-body system, as well as the disturbing accelerations due to the gravitational attraction of the bodies, can be studied and derived from the Newton universal gravitation law. The gravitational attraction of the bodies is obtained from the equation of the gravitational potential due to the presence of the third body, as a function of the gravitational constant, of the third body mass, and of the position of the bodies.
The lunar albedo is the fraction of solar energy reflected diffusely from the lunar surface into space, measured from the Moon's surface reflectivity. The perturbation model caused by the perturbations was based on the reflectivity of the Moon surface, due to variations in the lunar soil composition.
The perturbation model due to solar radiation pressure has been developed based on the albedo model. Considering that for the albedo model is necessary the modeling of the movement of the Sun, as well as the radiation that reach the spacecraft, and also the motions of the Moon and the satellite, some routines were implemented to provide these parameters to the albedo model and also to the solar radiation pressure model. However, it should be considered that the solar radiation reaches directly the satellite surface, instead of considering that solar radiation was reflected by the Moon's surface before reaching the satellite, such as considered in the albedo model.
In the proposed study, which analyzes the magnitude of the main disturbances that act on an artificial satellite around the lunar surface, was adopted an approach using the integration of forces alone, but simultaneously. Thus, the contributions of each disturbance are determined and then added to obtain the total disturbance acting on the satellite. Thus, it was possible to analyze the variation of the satellite orbital elements over the time. The control system used in the simulation was able to minimize the effects caused by disturbance, performing correction maneuvers and also performing the transfer maneuver, allowing analyses related to time and to the fuel consumption, for cases with an without correction maneuvers.

2. Methodology

For the realization of the study were developed numerical models of the main disturbing forces acting on a lunar artificial satellite. Such models were implemented into a trajectory simulator (STRS) and the proposed analyzes were made.
The description of the disturbing forces studied, as well as the developed models and the trajectory simulator utilized, is presented below.

2.1. Spacecraft Trajectory Simulator

All perturbations are studied, modeled and implemented in a simulator developed by Rocco 2008, called Spacecraft Trajectory Simulator - STRS, which allows controlling the trajectory so that deviations and errors in the state variables are minimized.
The simulator operates with a few specific characteristics: considers a closed loop control system, operating in a discrete manner in order to reduce to the maximum the state errors (position and velocity), utilizing continuous thrust. Thus, the state is determined and controlled at every simulation step to accomplish the orbital maneuver as required by the guidance subsystem.

The Figure 1 shows a block diagram representing the control system of the orbital trajectory in closed loop, used by STRS.
Initially, a reference state (Xref) must be defined. The reference state corresponds to the trajectory to be followed by the satellite to meet the goals of the mission. This reference is compared with the current state of the satellite (Xdet), which is obtained by means of sensors. This comparison generates an error signal, which is the input of the controller. The controller uses the PID techniques (proportional, integral and derivative gains) to generate the control signal that will be sent to the actuators, defining the magnitude and the direction of the velocity corrections to be applied. In the sequence, the output signal of the actuator model is added to the external orbital disturbances. Finally, this signal (the added actuator and disturbances signals) is considered by the dynamics of the orbital motion, determining the current position and velocity of the satellite. Through sensors and estimation algorithms, the current state of the satellite (Xdet) is obtained. To close the control loop, Xref and Xdet are compared, which generates an error signal, and the control cycle starts again.

2.2. Orbital Dynamics

The dynamics of orbital motion can be determined by solving the equation of Kepler every step defined as an input parameter in the simulator (STRS).
Given an initial state and a time interval, by solving the inverse problem of a positioning satellite it is possible to determine the keplerian elements of the orbit. Using Kepler's equation the keplerian elements are propagated for the time interval considered as input for the simulation. From the new keplerian elements, it is possible to obtain the propagated state by solving the direct problem of satellite positioning (Chobotov, 1991), as shown in Fig. 2.

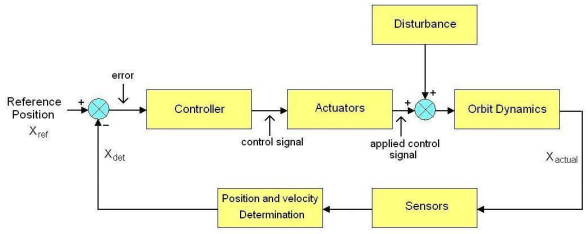

Figure 1. Trajectory closed loop control

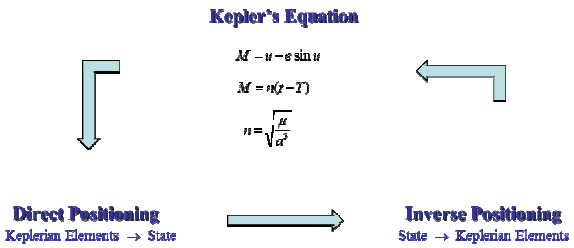

Figure 2. Dynamics of orbital motion

2.2. Perturbations and Models

A theoretical study of the major orbital perturbations that affect the motion of a lunar artificial satellite was made firstly. Then the model of each of these perturbation forces was developed and implemented into a trajectory simulator (STRS).
A brief explanation of each disturbance studied is presented below.

2.2.1. Potencial Gravitacional Lunar

The approach used to model the disturbance generated by the lunar potential was made from a study evaluating the influence of the lunar gravitational potential, modeled by spherical harmonics. This approach was used according to the model presented by Konopliv (2001).

The gravitational potential of the moon is expressed by the coefficients of the normalized spherical harmonics, given by Eq. 1 (Konopliv et al., 2001; Kuga et al., 2011):

$$U(r,\lambda,\phi) = \frac{\mu}{r} + \frac{\mu}{r}\sum_{n=2}^{\infty}\sum_{m=0}^{n}\left(\frac{a_e}{r}\right)^n (\bar{C}_{nm}\, cos\, m\lambda + \bar{S}_{nm}\, sen\, m\lambda)\bar{P}_{nm}(sen\, \phi) \quad (1)$$

where n is the degree, m is the order, μ is the gravitational constant and r is the orbit lunar equatorial radius. $\bar{P}_{nm}$ are the fully normalized associated Legendre polynomials; a_e is the reference radius of the Moon, ϕ is the latitude, and λ is the longitude.

The lunar gravity field was determined using data from different lunar missions already undertaken.
The data for the development of LP100K model were obtained by one of the most important missions, the Lunar Prospector (1998-1999), the third mission of Discovery space shuttle, NASA's exploration program, which made the first measurement of the Moon gravitational field. Since the epoch of the development of the LP100K model with the Lunar Prospector, no direct observations of the Moon far side have been made. The knowledge of the lunar gravitational field was obtained by observation of the long-term effects in a lunar artificial satellite orbit.
The LP100K model presented by Konopliv is a representation of spherical harmonics due to gravity planetary based on the gravitational potential of the celestial body, given by Eq. 1.
The output calculated by the model provides the components x, y and z for the gravity acceleration at each instant of time along the orbit of an artificial satellite. It is able to consider the spherical harmonics up to degree and order 100. By comparison between the gravity acceleration of a central field and the gravitational acceleration provided by Konopliv model, we obtain the disturbing velocity increment on the satellite. It is possible, by means of the solution of the inverse problem, to obtain the keplerian elements that characterize the orbit, so that the analysis of the orbital motion can be performed.
Studies analyzing the influence of no homogeneity of the lunar gravitational field on the orbit of Some studies analyzing the influence of non-homogeneity of the lunar gravitational field on the orbit of an artificial satellite, can be found in Gonçalves et al., 2013a: considering the contribution of each term of the potential; considering the disturbance as a function of the orbit inclination; considering the actuation of the control system in order to minimize perturbation effects on the orbit.

2.2.2. Atração Gravitacional da Terra e do Sol

Taking into account the presence of a third body the function of the gravitational potential is given by Eq. 2 (Chobotov, 1991), where μ' is the gravitational constant multiplied by the mass of the third body, r' is the module of the position vector of the third body; is the angle between the position vector of the satellite relative to the Moon and the position vector of the satellite relative to the third body; r is the module of the satellite position vector with respect to Moon.

$$F' = \left(\frac{\mu'}{r'}\right)\left[1 + \sum_{n=2}^{\infty}\left(\frac{r}{r'}\right)^n P_n \cos\psi\right] \quad (2)$$

The general problem of three bodies presented by Szebehely, 1967, and used by Prado and Kuga, 2001, provides the Eq. 3 to calculate the disturbing accelerations due to the gravitational

attraction of the bodies, where: $\vec{r}_1$, $\vec{r}_2$ e $\vec{r}_3$ are the positions of bodies, m_1, m_2 e m_3 are the masses of bodies and G is the gravitational constant.

$$\begin{aligned}
\ddot{\vec{r}}_1 &= -Gm_2\frac{\vec{r}_1-\vec{r}_2}{|\vec{r}_1-\vec{r}_2|^3}+Gm_3\frac{\vec{r}_3-\vec{r}_1}{|\vec{r}_3-\vec{r}_1|^3}\\
\ddot{\vec{r}}_2 &= -Gm_3\frac{\vec{r}_2-\vec{r}_3}{|\vec{r}_2-\vec{r}_3|^3}+Gm_1\frac{\vec{r}_1-\vec{r}_2}{|\vec{r}_1-\vec{r}_2|^3}\\
\ddot{\vec{r}}_3 &= -Gm_1\frac{\vec{r}_3-\vec{r}_1}{|\vec{r}_3-\vec{r}_1|^3}+Gm_2\frac{\vec{r}_2-\vec{r}_3}{|\vec{r}_2-\vec{r}_3|^3}
\end{aligned} \tag{3}$$

2.2.3. Albedo Lunar

The lunar albedo is the fraction of solar energy reflected diffusely from the lunar surface into space, measured from the surface reflectivity of the Moon, Eq. 4. Then:

$$albedo = \frac{radiation\ reflected\ to\ the\ space}{incident\ radiation} \tag{4}$$

The possible values for the lunar albedo can range from 0 (completely opaque) to 1 (fully bright) and depend of the surface conditions.
The albedo effect of the artificial satellite can vary depending on some factors: the satellite position, the satellite attitude, and the optical properties of the satellite surface.
The solar radiation includes all electromagnetic waves emitted by the Sun. The radiation incident with a right angle in an area of 1 m² at a distance of 1 AU (149598200 ± 500 km) is 1371 ± 5 W/m², which is known as the solar constant (Stark, 1994). The solar radiation of a distance d is given by Eq. 5:

$$J_S = \frac{P}{4\,\pi\,d^2} \tag{5}$$

where P is the total energy emitted by the sun (3.8 x 10^{25} W) and d is the distance from the satellite to the Sun.

The reflectivity of each point of the Moon surface is calculated by measuring the amount of radiation received by the satellite, given by Eq. 6:

$$E_C = \frac{\rho\, f}{1 - S\,\rho}\, E_{AM0} \tag{6}$$

where: ρ is the reflectivity of the reflector surface; f is the fraction of the reflected radiation that reaches the satellite; S is the fraction of the reflected radiation scattered back to the surface reflective; $\mathrm{E_{AM0}}$ is the amount of the radiation that reaches the reflective surface.

Considering that Moon does not have atmosphere $f = 1$ and $S = 0$. Thus, for the Moon case, the Eq. 6 reduces to Eq. 7:

$$E_C = \rho\, E_{AM0} \tag{7}$$

More details and explanations can be found in Rocco, 2008.
The model of the perturbation caused by the lunar albedo was based on the reflectivity of the Moon surface.
Due to the variation of the reflectivity of the lunar soil, the moon surface was divided into cells allowing studying the behavior of incident light in each cell. The incident light on the Moon reflected by each cell is used to calculate the total flux incident on the satellite surface. Such

radiation on the satellite is calculated using as base the model developed by Rocco 2008, who studied the behavior of the terrestrial albedo.
The amount of cells, and also the dimensions of the cells, can vary from one cell and the maximum of 51840 cells. Taking into account the maximum number of cells, the dimension of each is 1.25 degree of longitude and one degree of latitude.
To consider the effect on the satellite orbit due to the solar radiation reflected on the Moon surface, it is necessary to know the positions of the Sun, Moon and the satellite, whose movement was modeled and inserted in the simulator.
For each cell is assigned a value for reflectivity: 1 represents the complete reflection of the incident light and 0 represents the total absorption, in other words, white cells receives values near to 1 and the black cell receives values near to 0.
Thus, initially it is made an analysis of the Moon image, in a way that for each division is assigned values for the reflectivity, but first it is necessary to convert the image to a degree of gray. Then a calibration is done in the image brightness so that the value of the average of the reflectivity is coincident with to the medium albedo of the Moon, which is 0.12.
The calibrated image was divided into cells. A routine was used to calculate the average of the brightness of the pixels in each cell. Thus it might be assigned a value corresponding to the albedo for each cell, to thereby be generated the reflectivity matrix of the Moon surface.
The reflectivity matrix of the Moon, as well as an analysis of the influence of the number of cells on the accuracy of the disturbance due to the lunar albedo and its effect on the trajectory of a lunar artificial satellite can be found in Gonçalves et al., 2013b.

2.2.4. Pressão de radiação solar

The solar radiation pressure is a non-gravitational force able to disturb the translational motion of a lunar artificial satellite due to the momentum of the photons that strike the satellite surface, causing a variation in the orbital elements.
The rate of change of radiant energy per unit of area is given by Eq. 9.

$$\left(\frac{\frac{d}{dt}(E)}{dA}\right) = \frac{P}{dA} \tag{9}$$

The radiant energy flow is proportional to the square of the heliocentric distance. Then, Eq. 10:

$$\bar{S} = S_0 \left(\frac{a_s}{R'}\right)^2 \tag{10}$$

where $\bar{S}$ is the radiant energy flow, S_0 is the solar constant.

And R 'is heliocentric distance from the surface affected by the flow, given by Eq.11:

$$p = \frac{\bar{K}}{R'^2} \tag{11}$$

where $\bar{K} = \frac{S_0 a_s^2}{c} = 1{,}01\ x\ 10^{17}\ kg\ m/s$ (Zanardi, 1993) and considering the pressure of solar radiation when the radiant energy flow is perpendicular to the surface in question is given by Eq. 12.

$$p = \frac{\bar{S}}{c} \tag{12}$$

and c being the velocity of light in vacuum.

In this work the model of the disturbance due to solar radiation pressure was developed based on the albedo model. Considering that is required to model the Sun movement, as well as its emitted radiation, and the Moon and the satellite's movement, for the albedo model, these same subroutines are also used to calculate the solar radiation pressure. However, it should be considered that the solar radiation directly reaches the satellite surface, instead of considering that solar radiation was reflected by the surface of the Moon before reaching the satellite, as in the albedo case.
Models of solar radiation pressure can be found in Vilhena de Moraes (1978) and Zanardi (1993) and the application of the model used in this study showing the influence of solar radiation pressure and lunar albedo in the orbital elements of an artificial satellite around the Moon for different values of altitude and inclination can be found in Gonçalves et al., 2014a.

3. Simulations and Results

As mentioned earlier, the aim of this work is divided into three stages. The first is to analyze the magnitude of the main orbital perturbations capable of altering the orbit of an artificial lunar satellite.
For this analysis was chosen the Lunar Prospector mission during the phases in which orbited the Moon. The Table 1 shows the initial orbital elements for each phase of the orbital maneuvering performed to insert the satellite in alunar orbit. These data can be found in Lozier et al., 1998

Table 1. Initial conditions - Lunar Prospector Mission

	Fase 1	Fase 2	Fase 3	Fase 4
a (km)	6014.6	2712.2	1860.4	1838.3
e	0.69714	0.32713	0.01653	0.00046
i (deg)	89.72	89.87	90.01	90.55
Ω (deg)	192.59	192.49	192.39	192.76
ω (deg)	150.37	150.32	147.86	224.02
M (deg)	10.63	90.13	59.16	317.04

Source: Lozier et al., 1998

The magnitude of the integral of each of the disturbing forces for different types of orbits has been studied in Gonçalves et al., 2014b, which showed the importance of each proving that none of them can be neglected.
In this paper, for each phase, during a one orbit around the lunar surface, it was obtained the magnitude of the integral of each perturbative forces due to the lunar gravitational potential, the gravitational attraction due to the Earth and the Sun, the lunar albedo and solar radiation pressure. It is noteworthy that for this study were not performed transfer and correction maneuvers. The results are shown in Tab. 2.

Table 2. Perturbative Forces

	Fase 1	Fase 2	Fase 3	Fase 4
Gravitational potential (N)	297.004	467.130	1001.374	1036.272
Earth attraction (N)	8.256	0.980	0.367	0.411
Sun attraction (N)	6.110	0.668	0.243	0.235
Albedo (N)	5,479	1.659	0.943	0.926
Radiation pressure (N)	0.403	0.470	0.561	0.560

We can see in all the phases an expected domain of the lunar gravitational potential, which tends to increase as the satellite approaches of the lunar surface.
Intuitively, it was expected that the albedo increase with the approach of the satellite and the Moon. But these were not the found results.
As explained in the item 2.2.3 of this work, to the satellite suffer disturbance due to the lunar albedo, solar radiation should focus on the Moon's surface and the portion of the reflected radiation should reach the satellite. A satellite at a high altitude can see a greater number of points illuminated by the Sun under the Moon surface than a satellite at a low altitude. This fact justifies the result obtained showing a higher albedo intensity in the early stages of the mission Lunar Prospector.
The second part of the work is to find the velocity increment to be applied on the satellite to perform the transfers maneuvers that connect the phases of the Lunar Prospector mission.
For this was utilized the Lambert's problem (Two Point Boundary Value Problem), to calculate and select an optimal ideal bi impulsive maneuver with respect the fuel consumption (minimum velocity increment). The results were organized in Tab.3 , where the Maneuver 1 is the maneuver performed to connect the phase 1 with the phase 2, the Maneuver 2 is the maneuver performed to connect stage 2 to stage 3 and the Maneuver 3 is the maneuver performed to connecting stage 3 to stage 4.
A detailed study and the algorithm for calculating of the maneuver can be found in Battin, 1999; Bond, 1996; Bate et al., 1971. This study can also be found in Rocco2014a and Rocco, 2014b, for the cases of an artificial satellite orbiting the Mars surface.

Table 3. Transfers Maneuvers

	Maneuver 1	Maneuver 2	Maneuver 3
Impulse 1	(-125,691, 2,659, 214,813)	(-113,602, 22,054, 204,130)	(54.425, -850.501, 207.531)
Impulse 2	(-4,260, 18,221, 0,807)	(-1,794, 7,959, 1,235)	(60.175, -837.322, 200.070)

The impulses calculated using the Lambert's problem have been entered as input parameters in the simulator STRS in order to accomplish the transfer maneuvers that connect each stage of Lunar Prospector mission.
Were considered two situations: the first in which it is performed an impulsive maneuver, which is an idealization because we consider that the velocity is instantaneous, and the situation in which we consider the non-impulsive case for different capacity of the thruster.
The results obtained for the errors in the orbital elements that characterize the orbit of the artificial satellite at each stage of the mission were organized in Table 4.

Table 4. Keplerian Elements Error and Propellant Consumption

	Impulsive					
	a (m)	e	i (deg)	Ω (deg)	ω (deg)	Propellant (kg)
Manobra 1	-8.076	-2.321	0.001	0.002	0.060	0.004
Manobra 2	2794.459	0.0007	0.315	-0.435	0.784	0.009
Manobra 3	-25.642	-0.0002	0.023	0.0342	-50.780	0.022
	150 N					
	a (m)	e	i (deg)	Ω (deg)	ω (deg)	Propellant (kg)
Manobra 1	-45455.326	-0.012	0.096	-0.100	5.207	3.656
Manobra 2	-11181.700	-0.021	0.322	-0.467	48.448	3.296

	200 N					
	a (m)	e	i (deg)	Ω (deg)	ω (deg)	Propellant (kg)
Manobra 1	-23220.003	-0.006	0.075	0.283	4.149	3.791
Manobra 2	-1094.537	-0.013	0.343	-0.495	48.241	3.383
	250 N					
	a (m)	e	i (deg)	Ω (deg)	ω (deg)	Propellant (kg)
Manobra 1	-10407.207	-0.003	0.023	0.244	3.439	3.909
Manobra 2	4046.312	-0.008	0.345	-0.476	46.770	3.430
	300 N					
	a (m)	e	i (deg)	Ω (deg)	ω (deg)	Propellant (kg)
Manobra 1	-5716.926	-0.002	0.008	0.207	2.909	3.988
Manobra 2	4667.637	-0.006	0.362	-0.546	42.620	3.528
	350 N					
	a (m)	e	i (deg)	Ω (deg)	ω (deg)	Propellant (kg)
Manobra 1	1412.670	0.0002	0.008	0.170	2.543	4.063
Manobra 2	10502.628	-0.003	0.371	-0.535	45.028	3.596

We can see that the effect of a propulsive arc is not the same as the application of an impulse. This difference causes deviation in final orbit of the satellite when compared with the reference orbit.

In the present work was considered the variation of thruster between 150 N, 200 N, 250 N, 300 N and 350 N. In the case of the Maneuver 3, the great maneuver was calculated, but was found that it is not applicable to thrusters with a capacity below 500 N. A comprehensive study of the possibilities of maneuvers to connect the phases 3 and 4 may be made, but this approach is not the objective of this work.

To illustrate the variation of the thrust applied on the satellite for the non-inpulsive case, when varied the maximum propulsion adopted, only in case of the Maneuver 1, are shown in Figs. 3 to 7. The thrust applied to the satellite objective perform the maneuver transfer that connects the phase 3 to phase 4 of the mission, and realize correction maneuvers, which aims to minimize the effects of perturbative forces.

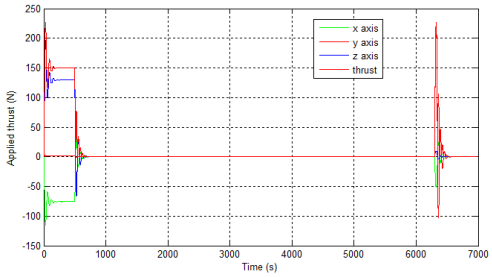

Figure 3. Applied thrust (150N)

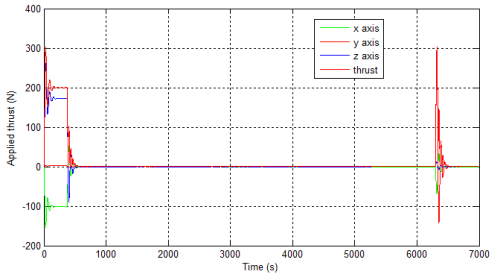

Figure 4. Applied thrust (200N)

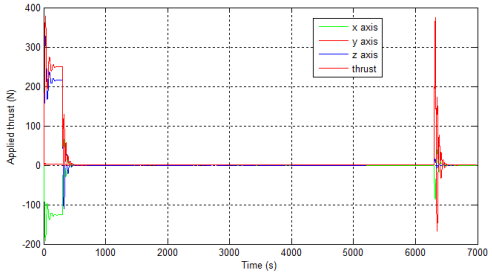

Figure 5. Applied thrust (250N)

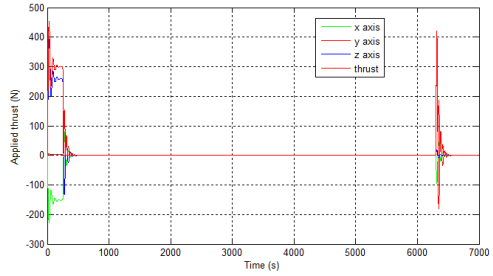

Figure 6. Applied thrust (300N)

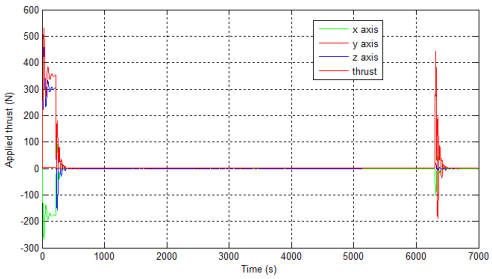

Figure 7. Applied thrust (350N)

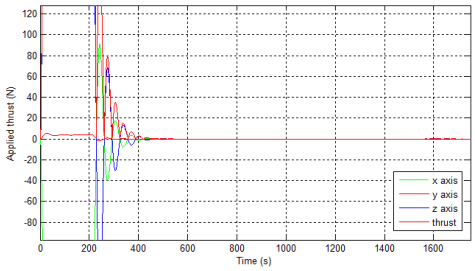

Figure 8. Transitional regime of the control system

It is worth noting that here is being presented a theoretical study, they are not in use actual values for the thrust applied by the thrusters.

We can see clearly the non-impulsive cases presented high errors for the orbital elements, and the impulsive case presents satisfactory values for the error.

The high values for the error introduced by non-impulsive cases is due to the fact that the thrust capacity is not infinite, and the velocity calculated by the Lambert's problem is distributed in a propulsive arc, generating errors. The velocity should be applied at one point, not in an arc.

It is possible to see that as we increase the magnitude of the thrust is reduced the size of the propulsive arc, and that the thruster is not abruptly turned off. The control system turn off the thruster with fluctuations which decrease the thrust, until it is totally turned off, due to transitional regime, shown from Figure 7 and shown in Figure 8.

To solve the problem of maneuvering a lunar artificial satellite, some options are possible: the use of several small propulsive arches, splitting the maneuver in many small maneuvers applied in consecutive orbits; calculate the maneuver for each point of the trajectory changing the direction of the applied thrust, which requires an attitude control system; another option is to keep the thrust direction fixed, which ends up introducing a very big path error; or you can use an automatic control system for the trajectory, making the control continuously, in a way that the error in the trajectory is analyzed incessantly, trying to reducing the error at each instant of time until the desired final orbit is reached, without the necessity of applying the maneuver provided by the TPBVP. With the automatic approach is not necessary to calculate the maneuver, or even the correction, because the automatic control system alone is capable to define the magnitude and direction of the thrust necessary to transfer the vehicle to the desired final position.

Then, to complete the study proposed for this work, we used an automatic control system to perform the maneuver 3, which transfers the satellite from the phase 3 to phase 4 and minimizes the effects of perturbations in the orbit.

For this work the control system has acted on the semi-major axis and the eccentricity, whose deviations are shown in Figs. 9 and 10, and the thrust applied on the satellite is shown in the Fig. 11.

The problem of controlling all orbital elements simultaneously may be supposed to be a multi-objective problem, since to correction one element leads to change in others. The simultaneously control of all orbital elements using continuous thrust, in case of an artificial satellite in Earth orbit, can be found in Rocco, 2012.

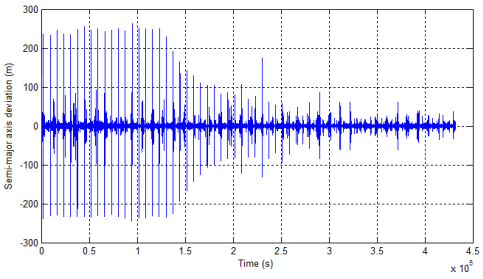

Figure 9. Semi-major axis deviation

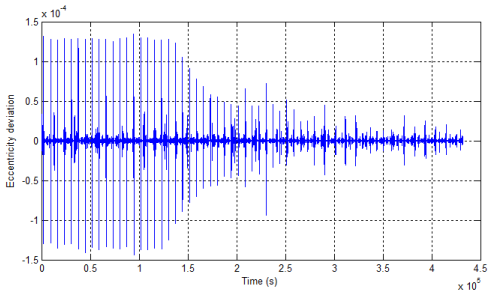

Figure 10. Eccentricity deviation

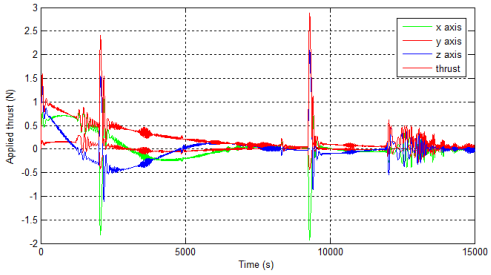

Figure 11. Applied thrust (automatic control)

By the Figs 9 and 10 we can see that the control system could transfer the satellite from the initial conditions of phase 3 to initial conditions of phase 4, minimizing the effects caused by disturbances and keeping the satellite close to its reference trajectory, with fuel consumption of 1.373 kg.

4. Conclusions

The problem of analyzing the magnitude of the perturbative forces due to lunar gravitational potential, gravitational attraction of the Earth and the Sun, lunar albedo and solar radiation pressure was accomplished and showed that the lunar gravitational potential exerts greater influence than all other forces, even if added together, regardless of any initial conditions.

The approach of the Lambert's problem was sufficient to quantize the magnitude of the pulses to be applied on the artificial satellite to perform the necessary maneuvers to connect each one of the four phases of the Lunar Prospector. However this approach is an ideal and utopian solution, which is not applicable in practice because it requires the instantaneous velocity change, and hence, infinite thrusters capacity, which is impossible to achieve in the real world.

We also observed that the effect of a propulsive arc on the deviation of the orbital elements is greater than case when an impulse is applied. In general, this deviation decreased with the increasing of the magnitude of the thruster.

To solve the problem of maneuvering the satellite of the Lunar Prospector mission, it was proposed an innovative technology with automatic correction that reduces errors in the variables of the satellite orbit. The system that uses continuous propulsion and trajectory control in closed loop has been tested and has achieved the stipulated transfer maneuver and also was capable to apply the correction maneuvers to reduce deviations in the orbital elements caused by the perturbative forces considered in this study.

5. References

[1] Chobotov, V. A, "Orbital Mechanics", p 365, 1991.

[2] Gonçalves, L. D., Rocco, E. M., de Moraes, R. V. and Prado, A. F. B. A. "Study of the potential effects on Lunar Spacecraft Trajectories" (in Portuguese). XI Conferência Brasileira de Dinâmica, Controle e Aplicações, Fortaleza, Brasil, 2013a.

[3] Gonçalves, L. D. "Evaluationofthetrajectorydeviationof a spacecraftduetothe lunar albedo." Congresso Brasileiro de Engenharia Mecânica, Ribeirão Preto, Brasil, 2013b.

[4] Gonçalves, L. D., Rocco, E. M., de Moraes, R. V. " Studies of Solar Radiation Pressure Effects and Lunar Albedo in the Orbital Motion of an Artificial Satellites" (in Portugueses). VIII Congresso Nacional de Engenharia Mecânica. Uberlândia, Minas Gerais, Brasil, 2014a.

[5] Gonçalves, L. D., Rocco, E. M., de Moraes, R. V. "Influence Analysis of Perturbative Forces of Gravitational and Non-Gravitational Origin in Lunar Artificial Satellites" (in Portuguese). Congresso Brasileiro de Dinâmica Orbital. Águas de Lindóia, São Paulo, Brasil, 2014b.

[6] Konopliv, A. S.; Asmar, S. W.; Carranza, E.; Sjogren W. L.; Yuan, D. N. "Recent gravity models as a result of the lunar prospector mission" .Icarus, Vol. 150, pp. 1-18, 2001.

[7] Kuga, H. K., Carrara, V. and Kondapalli, R. R. "Artificial Satellites - Orbital Motion" (in Portuguese). INPE Available in: http://urlib.net/8JMKD3MGP7W/3ARJ3NH

[8] Lozier, D., Galal, K., Folta, D., Beckman, M. “Lunar Prospector Mission Design and Trajectory Support”, AAS 98-323, 1998.

[9] Prado, A. F. B. A., Kuga, H. K. "Space Technology Fundamentals" (in Portuguese) Instituto Nacional de Pesquisas Espaciais, São José dos Campos ISBN: 85-17-00004-8. 2001.

[10] Rocco, E. M. "Perturbed orbital motion with a PID control system for the trajectory". Colóquio Brasileiro de Dinâmica Orbital, Águas de Lindóia, São Paulo, Brasil, 2008a.

[11] Rocco, E. M. "The earth albedo model." Center of Applied Space Technology and Microgravity (ZARM), Bremen, Germany. Technical Report FLK-ENV-RP-ZAR-001, 91 p., 2008(b).

[12] Rocco, E. M. "Automatic correction of orbital elements using continuous thrust controlled in closed loop." Journal of Physics: Conference Series, doi:10.1088/1742-6596/465/1/012007, 2012.

[13] Rocco, E. M. "Simulation of the Effects due to the Gravitational Disturbances Generated by the Sun, Phobos and Deimos in Orbital Maneuvers around Mars." XXXV Iberian Latin American Congress on Computational Methods in Engineering. Fortaleza, Ceará, Brasil, 2014a.

[14] Rocco, E. M. "Gravitational Disturbances generates by the Sun, Phobos and Deimos in Orbital Maneuvers around Mars with Automatic Correction of the Semi-major Axis" Journal of Physics: Conference Series, 2014.

[15] Stark, J.; Fortescue, P. "Spacecraft Systems Engineering." 1994.

[16] Szebehely, V. "Theory of orbits." 1967.

[17] de Moraes, R. V. “Action of solar radiation pressure and atmospheric drag on artificial satellite orbits.” (in Portuguese) Doctorate thesis, ITA, São José dos Campos, 1978.

[18] Zanardi, M. C. F. P. S. “Influence of Solar Radiation Torque in the Attitude of an Artificial Satellite.” (in Portuguese) Doctorate thesis, ITA, São José dos Campos, 1993.